

# Application of Electron Paramagnetic Resonance for Evaluating and Improving the Mechanical Performance of Cement-Based Materials

Laith N. Ali<sup>1</sup><sup>\*</sup>

<sup>1</sup>Ministry of Higher Education and Scientific Research, Baghdad/ Iraq.

\*Corresponding Author: Laith N. Ali

DOI: <https://doi.org/10.55145/ajest.2026.05.01.014>

Received December 2025; Accepted January 2026; Available online February 2026

**ABSTRACT:** Cement-based materials play a vital role in modern construction, where mechanical performance and durability are of primary importance. This study investigates the microstructural and mechanical properties of Portland cement-based systems using electron paramagnetic resonance (EPR) spectroscopy in combination with compressive strength tests. The results indicate that an increase in the specific surface area of cement particles leads to a higher concentration of spin centers, which influences hydration processes and strength development. The addition of activated Portland cement in the range of 5–15 wt.% resulted in an improvement in compressive strength of up to 15%. However, a further increase beyond this range caused a reduction in strength, which may be attributed to decreased material density and less efficient particle packing. High-strength and rapid-hardening cements exhibited higher concentrations of spin centers and improved mechanical performance. These findings confirm that EPR analysis is a useful tool for evaluating the relationship between microstructural characteristics and the mechanical behavior of cement-based materials.

**Keywords:** Portland Cement, Electron Paramagnetic Resonance (EPR), Spin Centers, Compressive Strength, Cement-Based Materials, Civil Engineering Applications



## 1. INTRODUCTION

Cement is one of the main building materials and is widely used in the manufacture of concrete, reinforced concrete, asbestos-cement products, mortars, and many other artificial materials for various technical purposes. Improving the properties of cement with minimal energy consumption, as well as creating cement systems with unique properties, is considered one of the urgent tasks in cement chemistry [1,2]. Modern trends in the development of building materials science are associated with the transition toward multicomponent, multilayer, and multilevel composite materials with a given set of properties, their structural and functional organization, and behavior adapted to variable environmental factors throughout the entire service life, while at the same time preserving or improving the quality of the habitat. Achievement of these goals, in our opinion, is possible by following the principles of nonlinear chemistry, bionics [3], and geonics [4,5], according to which priority is given to naturally balanced, biosphere-compatible materials and technologies for their production. In this regard, new-generation concrete can be attributed to such materials [6]. Similar approaches aimed at enhancing the performance of cementitious materials with reduced energy consumption have been reported in previous studies [7,8]. A distinctive feature of the production of such cement systems is the consideration of the physicochemical capabilities of each component of concrete and building mixtures, the prehistory of their preparation and interaction, and the conscious choice of methods for their activation and modification by mechanical, physical, chemical, biological, and combined external influences [9,10]. Cement technology is characterized by the involvement of the latest achievements of modern chemistry and physics in describing hardening processes, including quantum mechanics, thermodynamics, synergetics, and solid-state physics. Among physicochemical research methods, several promising and successfully applied techniques can be distinguished in the study of cement systems, such as nuclear magnetic resonance (NMR), electron paramagnetic resonance (EPR), infrared (IR) spectroscopy, X-ray phase analysis (XPA), and scanning electron microscopy (SEM) [11,12]. Let us focus

on radio spectroscopy methods. The NMR method for studying cement systems has undergone rapid development over the past three decades, which is largely associated with the modernization of instrumentation, including increased sensitivity and resolution, as well as the discovery of new capabilities of these devices. To date, a large number of studies have been devoted to the investigation of cement systems using this method, whose main advantage is the isotope selectivity of nuclear spins ( $^1\text{H}$ ,  $^{13}\text{C}$ , etc.). The resonances of these nuclei selectively reflect corresponding structures, while amorphous and crystalline phases are identified with comparable efficiency, thereby complementing diffraction methods. NMR studies of cement systems can be divided into three main branches [13]:

- High-resolution magic-angle spinning (HR-MAS) NMR – obtaining structural and quantitative characteristics from  $^{29}\text{Si}$  and  $^{27}\text{Al}$  nuclei in anhydrous and hydrated cement phases;
- $^1\text{H}$  NMR – obtaining information on cement porosity and the amount of free and bound water;
- Magnetic resonance imaging (MRI) – studies at the  $\mu\text{m}$ – $\text{mm}$  scale to characterize pores, cracks, and water diffusion.

In comparison with other physicochemical methods, the use of EPR for studying cement systems remains relatively limited. Previous studies have demonstrated the applicability of EPR spectroscopy for investigating paramagnetic centers in clinker minerals and hydrated cement systems [14]. EPR spectrometers respond only to systems containing unpaired electrons and make it possible to detect and, in many cases, identify free radicals. The available literature on this topic is relatively scarce and is mainly focused on the artificial introduction of radicals or their generation by  $\gamma$ -irradiation, after which changes in radical characteristics (such as EPR line width, STS constants, etc.) are correlated with specific features of the system. This area of EPR spectroscopy is commonly referred to as the spin-label method. As early as the 1970s, studies on clinker minerals using EPR were published, involving the introduction of paramagnetic manganese particles or the generation of spin centers (SCs) by  $\gamma$ -irradiation, that is, by artificially inducing paramagnetism in the system [15].

Apparently, in [16], the presence of spin centers in dry cement systems was first recorded without additional impact on the system, and it was noted that SC of iron and manganese can be used as a spin label to study the processes of crystallization and solidification of cement paste. However, experimental material reflecting the kinetics of the hardening of binders using a spin label is presented in [17], where it was suggested that radical processes are taking place. It was also found that the introduction of substances that generate free radicals leads to an increase in the strength of the cement stone. Apparently, the researchers were the first to emphasize the possibility of radical processes during the hardening of cement. In addition, the article notes that chemical reactions proceeding by a radical mechanism for a long time are difficult to detect by direct radio spectroscopy of cement samples, while a device for recording an electron paramagnetic resonance (EPR) spectrum should have high resolution and sensitivity. Similar relationships between paramagnetic characteristics and the mechanical performance of cement-based materials have been suggested in previous studies, indicating the role of radical and defect-related processes during hydration and hardening.

These studies emphasized the possibility of radical mechanisms during cement hardening. At the same time, it was noted that chemical reactions proceeding via radical mechanisms over long periods are difficult to detect by direct radio spectroscopy of cement samples, and that EPR instruments used for such studies should possess high resolution and sensitivity.

However, practical observations show that in cements the total number of spin centers can reach  $10^{20}$ – $10^{22}$  spin/g [18]. In EPR spectra, these centers usually form a broad unresolved signal composed of a set of fine-structure lines. This makes it possible to study changes in the overall paramagnetic component of cement systems, that is, quantitative variations of all paramagnetic particles characterizing the system during hardening, by analyzing spectra over a wide magnetic-field sweep range using direct radio spectroscopy. Such an approach allows the identification of new correlations with the properties of the resulting material. From both scientific and practical perspectives, increasing the operating frequency and, accordingly, the magnetic field of the EPR spectrometer is of particular interest in order to obtain a more resolved spectral structure that reflects the specific nature of ongoing radical processes. In addition, for cement systems exhibiting characteristic hyperfine structure (HFS) in EPR spectra, the use of double electron–nuclear resonance (ENDOR) can be useful for identifying paramagnetic particles.

In this work, studies of cements and cement-based systems using EPR spectroscopy are continued and significantly extended. In particular, the analysis includes clinker materials, cement additives such as Polyplast SP-1 and SP-3/SP-4, and the influence of increasing the specific surface area of Portland cement M-400 to approximately  $18\,000\text{ cm}^2/\text{g}$  on the paramagnetic properties of particles and the phase composition of the material. Considering the individuality of EPR spectra obtained for cement systems, this method is proposed as an express technique for binder identification. In addition, the relationship between cement strength and spin characteristics is analyzed, and assumptions are made regarding approaches to producing high-strength cementitious materials.

Nomenclature is included if necessary  
 A radius of  
 B position of  
 C further nomenclature continues down the page inside the text box

## 2. EXPERIMENTAL METHODS

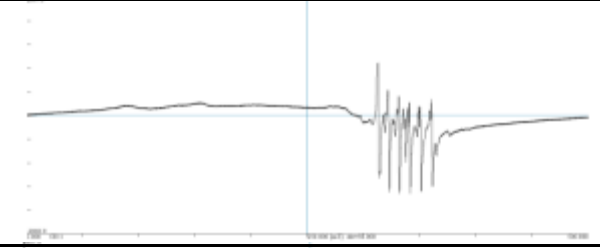
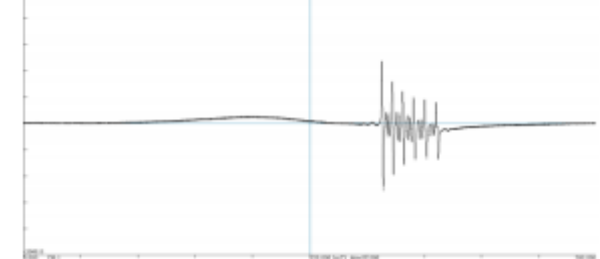
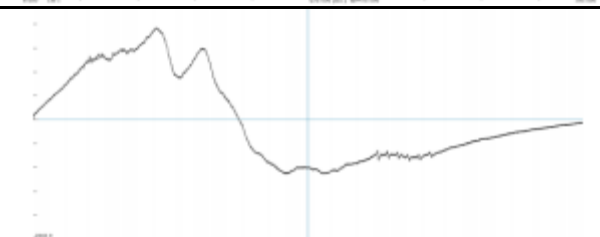
A complex of physicochemical research methods was used in this work, including EPR (electron paramagnetic resonance), ENDOR (double electron–nuclear resonance), XRF (X-ray fluorescence), and radio-frequency luminescence analysis (RFLA). The main research instrument was a JEOL JES-FA200 electron spin resonance spectrometer (also referred to as EPR), operating in the three-centimeter wavelength range with a microwave radiation frequency of approximately 9.4 GHz. The magnetic field sweep was carried out in the range from 0 to 500 mT.

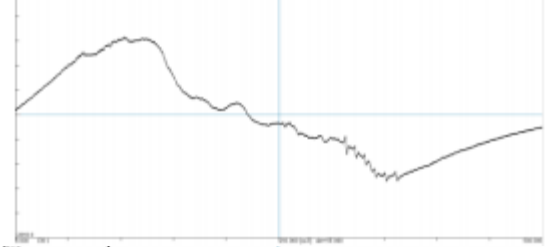
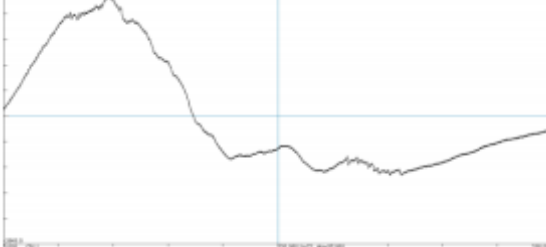
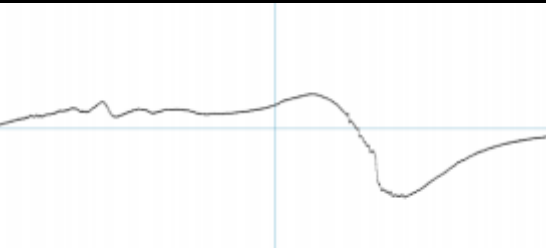
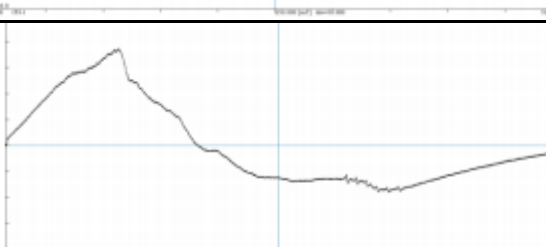
To calculate the amount of CSC, the shape of the first derivative of the EPR absorption line was analyzed, followed by integration and determination of the area under the curve using the standard application software supplied with the instrument. In order to perform more accurate quantitative measurements independent of the dielectric parameters of the sample, a ruby rod standard rigidly fixed in the resonator was used. Initially, the concentration of CSC in ruby was calculated based on the known concentration of a vanadium(IV) acetylacetonate sample,  $VO(acac)_2 = 5.50 \times 10^{20}$  spin/cm<sup>3</sup>. Subsequently, all calculations for the samples under study were performed relative to the ruby standard. To calculate the concentration of SC in spin/g, the bulk density expressed in g/cm<sup>3</sup> was used. The cement was mixed with distilled water at a water-to-cement ratio of 0.34. For the activated form of Portland cement and mixtures based on it, this ratio varied from 0.34 to 0.87. Curing of the cement samples was carried out under air-humid conditions.

## 3. RESULTS AND DISCUSSIONS

The EPR spectra of the main minerals and clays used in the production of cement are presented in Table 1.

**Table 1 EPR data for minerals and clays**

Sample name	Total concentration of spin centers, spin/g	Spectrum view
Gips "Ergach"	$3,46 \cdot 10^{20}$	
Limestone	$6,10 \cdot 10^{20}$	
Yellow clay	$9,22 \cdot 10^{21}$	

Brown clay	$3,73 \cdot 10^{21}$	
Variegated clay	$4,35 \cdot 10^{21}$	
Red-brown clay	$6,70 \cdot 10^{21}$	
Blue clay	$4,53 \cdot 10^{21}$	

The data of Table 1. Showed that the total concentration of CSC for these samples reaches values of the order of  $10^{21}$  spin/g.

The EPR spectrum of clay samples consists of an unresolved broad line and a weakly pronounced sextet in the  $g \sim 2$  region, obtained from the interaction of the magnetic moment of an electron of a paramagnetic particle with a nucleus with a spin equal to  $5/2$  (Al, Mg, Mn). The values of the corresponding  $g$ -factors are given in the Table 2.

**Table 2** Values of  $g$ -factors of the sextet line in the EPR spectra of clay samples

Sample name	g-factor					
Yellow clay	2,1536	2,0934	2,0363	1,9790	1,9246	1,8711
Brown clay	2,1535	2,0941	2,0362	1,9796	1,9241	1,8702
Variegated clay	2,1537	2,0950	2,0367	1,9788	1,9241	1,8713
Red-brown clay	2,1530	2,0946	2,0362	1,9799	1,9256	1,8716
Blue clay	2,1533	2,0942	2,0356	1,9798	1,9249	1,8704

For samples: limestone and gypsum "Ergach" The STS of the EPR spectrum is most likely the result of the interaction of the magnetic moment of an electron with more than one nucleus as illustrated in Table 1.

The EPR spectrum of "Ergach" gypsum in the range of 286 ... 386 MTL has a rather complex form, and the EPR spectrum of limestone in the range of 286 ... 386 MTL is a sextet, each line of which is clearly split into two. Perhaps this phenomenon is associated with the superposition of lines of hyperfine interaction formed from two different nuclei with a nuclear spin equal to  $5/2$ .

The study of the elemental composition by the XRD method (Table 3) showed that the sextet in the EPR spectrum was due to the presence of the elements Al, Mg, and Mn. Although the content of manganese in the samples is significantly lower than that of magnesium, the natural distribution of isotopes of these elements with  $I = 5/2$  equates their ability to form the HFS of the EPR spectrum. To solve such problems, i.e., to establish the nature of the nucleus

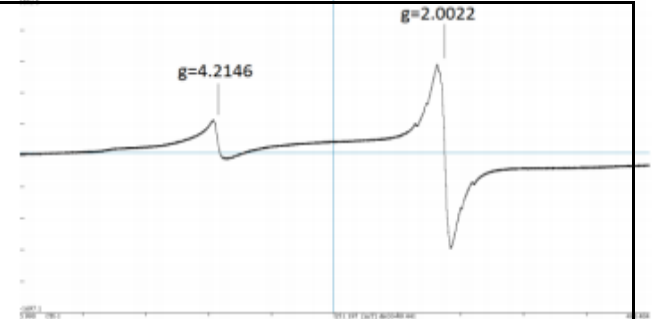
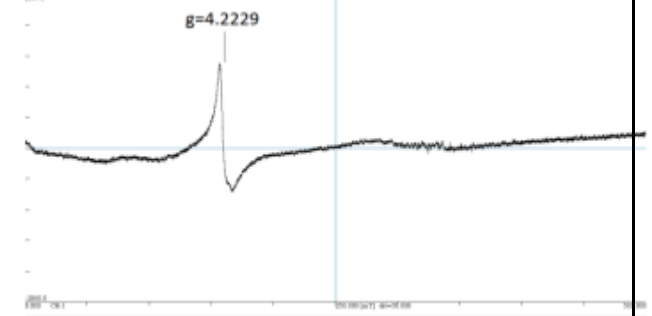
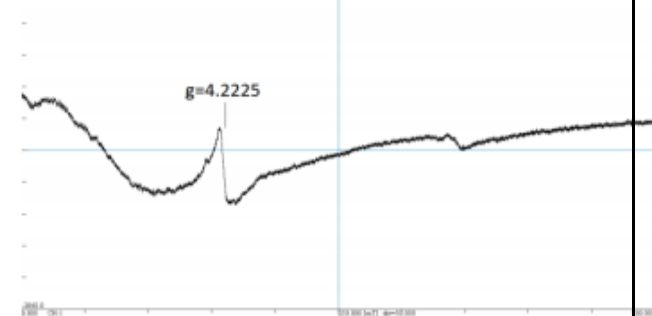
giving the HFS of the EPR spectrum, the ENDOR method can be used. However, the experiments carried out by the authors in this direction did not lead to success, since the intensity of the HFS lines of the EPR spectra of cement systems is not sufficient to obtain an adequate (double electron-nuclear resonance) (DENR) picture.

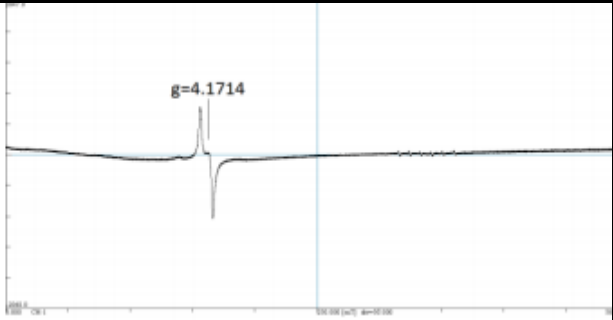
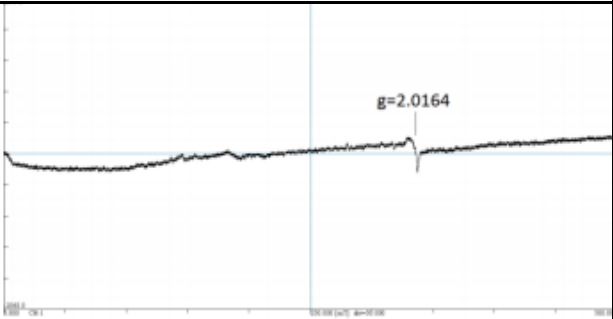
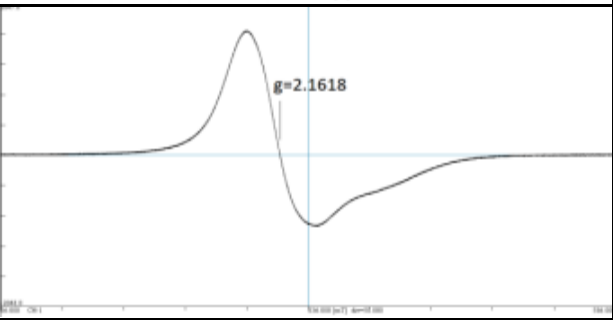
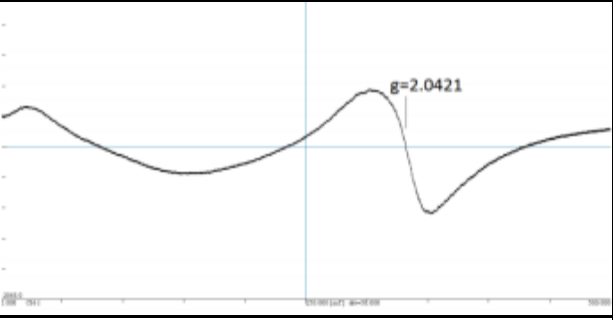
**Table 3 The quantitative content of some metals in the samples**

Metal	Metal content in the sample, wt. %		
	Limestone	Yellow clay	Gips "Ergach"
Mg	0,41	0,94	1,73
Ca	19,48	2,34	11,72
Al	0,34	3,38	0,28
Fe	0,56	2,73	0,28
Mn	0,01	0,06	0,01

The EPR spectrum of portland cement clinker, obtained by joint grinding of clay and limestone minerals with subsequent annealing, is characterized by two broad lines and a weakly pronounced sextet (Table 4). As you know, the main phases of Portland cement clinker are: tricalcium silicate, dicalcium silicate, tricalcium aluminate and calcium aluminoferrites [2]. EPR spectra of these minerals are also presented in the Table 4.

**Table 4 EPR data of clinker and clinker minerals**

Sample name	Spin center concentration, spin / g		Spectrum view
	S <sub>total</sub>	S <sub>4,2*</sub>	
Clinker bricks	$3,80 \cdot 10^{20}$	$3,12 \cdot 10^{18}$	
Tricalcium silicate	$3,22 \cdot 10^{18}$	$1,03 \cdot 10^{18}$	
Dicalcium silicate	$1,11 \cdot 10^{19}$	$3,71 \cdot 10^{17}$	

Tricalcium aluminate	$2,04 \cdot 10^{20}$	$2,72 \cdot 10^{18}$	
Monocalcium aluminate	$2,73 \cdot 10^{19}$	$7,03 \cdot 10^{16}$	
Dicalcium ferrite	$2,31 \cdot 10^{23}$	-	
Tetracalcium alumoferrite	$1,54 \cdot 10^{21}$	-	
*S <sub>4,2</sub> concentration of SC in the region g ~4,2			

The most paramagnetic minerals are dicalcium ferrite and tetra-calcium alumoferrite, the concentration of SC reaches  $2,31 \cdot 10^{23}$  and  $1,54 \cdot 10^{21}$ , respectively. For tricalcium aluminate, a weakly pronounced sextet is observed, the values of the corresponding g-factors are presented in the Table 5.

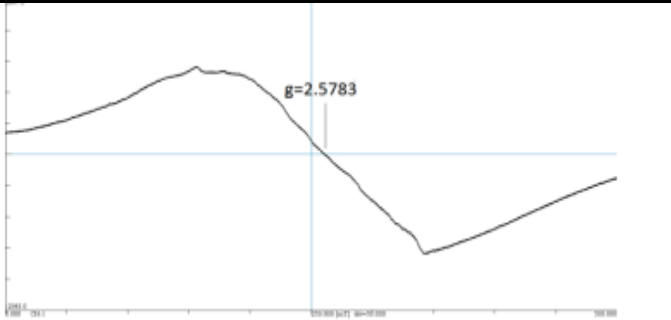
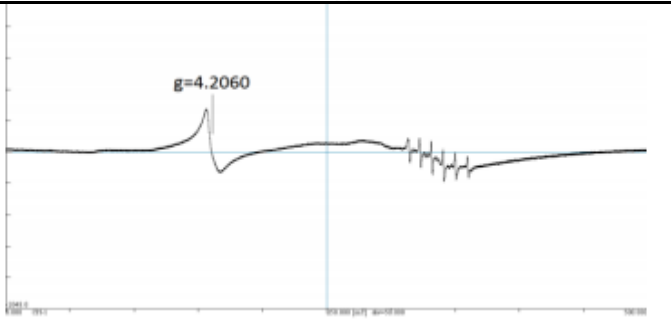
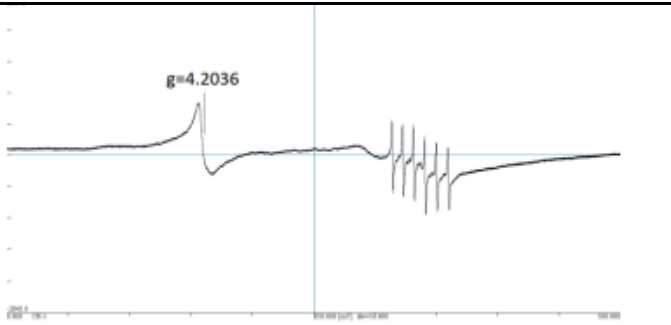
**Table 5** Values of g-factors of the sextet line in the EPR spectrum of tricalcium aluminate

g-factor					
2,1442	2,0881	2,0340	1,9806	1,9299	1,8797

EPR spectra of Portland cement and other cement systems are presented in the table 6. All cements are paramagnetic to one degree or another. The concentration of SC for these objects of study is 1019... 1022 spin/g.

**Table 6 EPR data of cements**

Sample name	Spin center concentration, spin / g		Spectrum view
	S <sub>total</sub>	S <sub>4,2</sub> *	
Portland cement M-400	$5,73 \cdot 10^{20}$	$4,26 \cdot 10^{18}$	<p>The EPR spectrum for Portland cement M-400 shows a complex signal with several peaks. Two prominent peaks are labeled 'рубин' (ruby) at approximately 1.5 and 2.5 T. The g-values for these peaks are 4.2178 and 2.0062, respectively. The x-axis represents the magnetic field in Tesla (T) from 0 to 100, and the y-axis represents the derivative of the absorption signal.</p>
Straining NC-10	$1,03 \cdot 10^{22}$	-	<p>The EPR spectrum for Straining NC-10 shows a broad, asymmetric peak centered around 2.6 T. The g-value for this peak is 2.6111. The x-axis ranges from 0 to 100 T, and the y-axis shows the derivative of the absorption signal.</p>
Gray building M-400	$1,64 \cdot 10^{21}$	-	<p>The EPR spectrum for Gray building M-400 shows a sharp, narrow peak centered around 2.0 T. The g-value for this peak is 2.0094. The x-axis ranges from 0 to 100 T, and the y-axis shows the derivative of the absorption signal.</p>
Expanding	$8,42 \cdot 10^{21}$	-	<p>The EPR spectrum for Expanding cement shows a broad, asymmetric peak centered around 2.8 T. The g-value for this peak is 2.7654. The x-axis ranges from 0 to 100 T, and the y-axis shows the derivative of the absorption signal.</p>
High-strength M-600	$9,60 \cdot 10^{21}$	-	<p>The EPR spectrum for High-strength M-600 shows a broad, asymmetric peak centered around 2.8 T. The g-value for this peak is 2.8386. The x-axis ranges from 0 to 100 T, and the y-axis shows the derivative of the absorption signal.</p>

Rapid hardening M-500 D-20	$1,01 \cdot 10^{22}$	-	
Turkish white M-500	$4,49 \cdot 10^{19}$	$2,71 \cdot 10^{18}$	
Shurovsky white M-500	$1,22 \cdot 10^{20}$	$4,65 \cdot 10^{18}$	

The EPR spectra of these cements can be divided into three groups according to the line shape:

1. With a wide line in the magnetic field range from 0 to 500 mT (cements: fast-hardening M-500 D-20, high-strength M-600, expanding, stressing NTs-10). Concentration SC 1021 ... 1022 spin/g.
2. With a weak or unresolved line in the region of  $g \sim 2$  and a weak peak in the region of  $g \sim 4.2$  (Cements: gray building M-400, Portland cement M-400). Concentration SC 1020 ... 1022 spin/g.
3. With a sextet in the area  $g \sim 2$  and a singlet in the area  $g \sim 4.2$  (Cements: Turkish white M-500, Shurovsky white M-500). Concentration SC 1019 ... 1020 spin/g.

In cement chemistry, one of the ways to increase the strength characteristics is to increase the specific surface area of the particles. In [7,8], it is noted that the mechanochemical process of grinding materials of silicate composition is accompanied by the destruction of the crystal lattice and the breaking of the siloxane bond (Si – O – Si), as a result of which  $O_2Si_2^-$  and  $O_3Si_3^-$  ions can form on the surface, which, in their turn, can be active centers of attachment. The question arises, how does the process of dispersing particles affect the concentration of SC?

Table 7 shows that the EPR spectra obtained under the same conditions (amplification, microwave power, etc.) of portland cement M-400 before activation (control) with a specific surface area of 3057 cm<sup>2</sup> / g and after activation (activated) with a specific surface area of 18130 cm<sup>2</sup>/g. As it can be seen, the process of increasing the specific surface area of the particles is accompanied by a significant increase in the total concentration of SC Portland cement. The elemental and phase compositions are shown in Table. 7 and Fig. 1 respectively. The phase composition after dispersion does not change, one can notice a decrease in the intensity of crystal reflections, and as a consequence, a decrease in the degree of crystallinity from 72% to 59%.

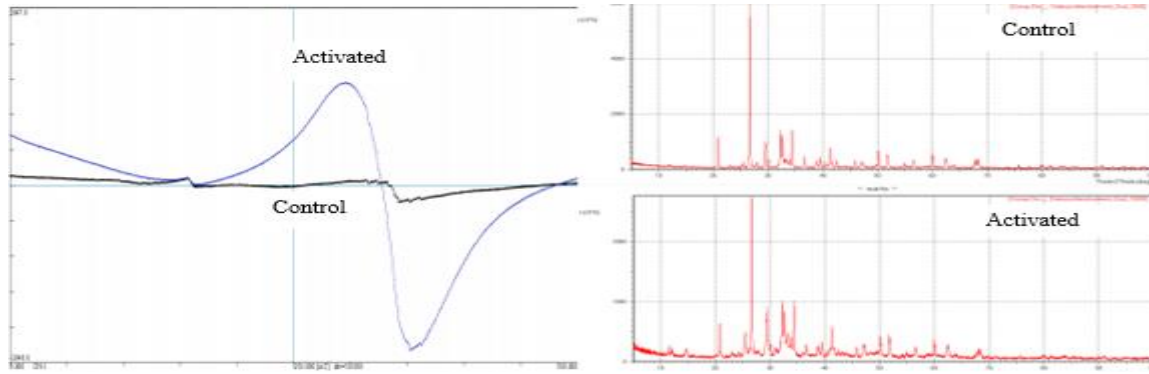


**FIGURE 1** Spectra of EPR and X-ray phase analysis of samples of Portland cement M-400 control and activated

**Table 7** Elemental composition of samples of Portland cement M-400 initial and activated

Element	Element content in the sample, wt. %	
	control	Activated
O	43,43	43,51
Ca	26,16	26,04
Si	24,08	20,45
Al	1,72	2,45
S	1,43	2,96
Fe	1,32	1,86
K	0,64	1,12
Mg	0,65	0,78
Na	0,26	0,31
Ti	0,16	0,22
Cr	0,05	0,08
Sr	0,05	0,06
Mn	0,04	0,05
P	0,03	0,06
C	0,03	0,05
Zn	0,02	0,03
Ni	0,02	0,02

The compressive strength of the activated form of Portland cement M-400 is significantly inferior to its control form at all studied setting times (Table 8). However, the addition of small amounts up to 10 ... 15% wt. activated form in the original Portland cement leads to an increase in its compressive strength up to 15%. Further increase more than 15% wt. the activated form is accompanied by a decrease in the compressive strength, which, apparently, is associated with a decrease in the density of the resulting cement stone. Adding the activated form up to 15% wt. leads to a slight loss of density, which is compensated by the high activity of the added particles.

After one day of hardening, the best result of compressive strength among the samples of Portland cement was shown by a sample with an activated form content of 15% wt. However, after curing for 7 and 28 days, the maximum values of the compressive strength correspond to samples with an activated form content of 10 and 5 wt% . respectively. These results are explained by the fact that in the initial setting time, the strengthening of the structure occurs mainly due to the activated fraction, and the further strengthening of the structure largely depends on the density of the resulting material, which decreases with an increase in the content of the activated form.

**Table 8** Values of compressive strength of cement systems for the hardening period of 1, 7 and 28 days

Type of cement	Compressive strength, kg / cm <sup>2</sup>		
	1 day	7 days	28 days
Control (K)	173	414	602
K+5%A	182	455	671
K+10%A	186	468	617
K+15%A	203	428	503
K+25%A	167	356	403
K+50%A	162	262	369
K+75%A	108	215	306
Activated (A)	86	143	214
High strength M600D0	260	663	722
Rapid hardening M500D20	148	682	724

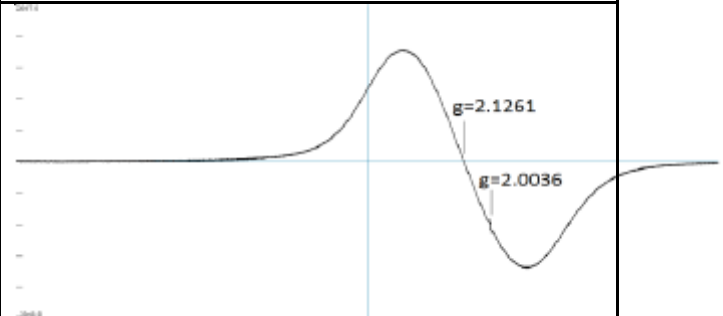
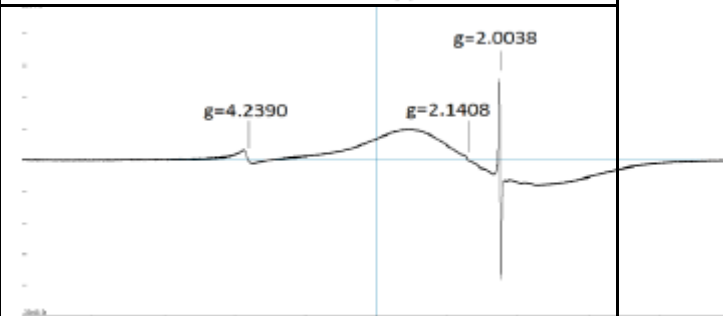
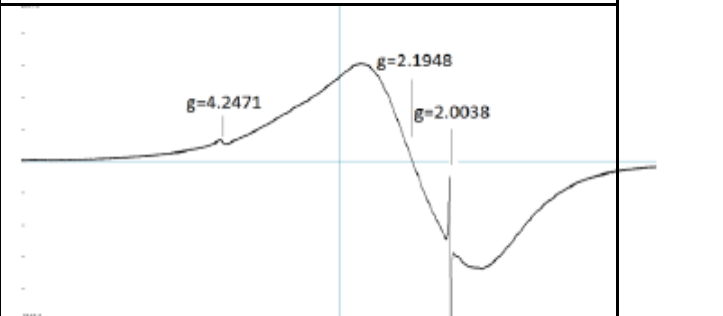
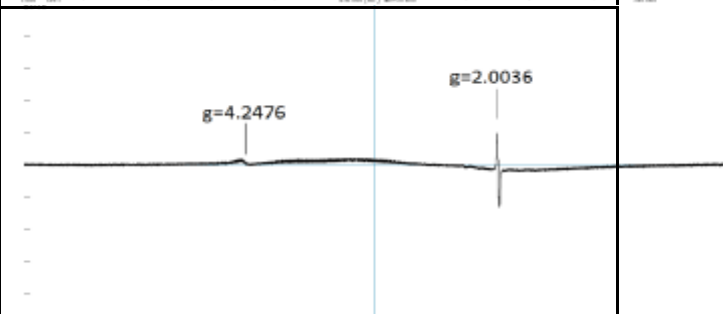
If we carry out a comparative analysis of the three characteristics of the studied cements: strength, density, and SC concentration, we can see that the cements with the maximum strength — the fast-hardening M500D20 and the high-strength M600D0 — are also characterized by the maximum density and the maximum value of the SC concentration (Table 9). Therefore, it can be assumed that in order to improve the strength characteristics of cement, all other things being equal, it is necessary to create a system with a high content of paramagnetic particles and sufficient density, which can be achieved by observing a certain particle size distribution according to the fuller curve [ 14].

**Table 9** Values of the concentration of spin centers of cement systems for the hardening period of 3, 14 and 28 days

Type of cement	Total concentration of paramagnetic centers, 10 <sup>21</sup> spin/g			
	Dry systems	3 days	14 days	28 days
Control (K)	0,39	0,72	0,45	0,31
K+5%A	0,68	0,73	0,74	0,64
K+10%A	0,88	1,14	0,93	0,79
K+15%A	1,25	1,13	1,03	1,03
K+25%A	1,62	1,36	1,32	1,25
K+50%A	2,45	2,12	1,95	1,91
K+75%A	3,64	2,75	2,68	2,44
Activated (A)	4,95	4,45	3,29	3,15
High strength M600D0	9,84	11,2	8,37	7,54
Rapid hardening M500D20	10,2	12,2	9,81	8,38

EPR spectra of the investigated additives - superplasticizers are given in the Table 10. As it can be seen, these compounds also have spin properties, the EPR spectra have similar features, namely: a narrow line in the  $g \sim 2$  regions, a wide line in the  $g > 2$  regions, and a line with a  $g$ -factor of  $\sim 4.2$ . For the cryoplast sp15-1 sample, the wide line in the  $g \sim 2.3$  region is less pronounced.

**Table 10 EPR data of additives – superplasticizers**

Sample name	Spin center concentration, spin / g		Spectrum view
	$S_{total}$	$S_{4,2}; S_2^*$	
Polyplast SP-1	$2,2.10^{21}$	–; $4,2.10^{15}$	
Polyplast SP-3	$1,3.10^{20}$	$6,6.10^{17}$ ; $4,2.10^{16}$	
Polyplast SP-4	$3,2.10^{20}$	$1,2.10^{16}$ ; $3,2.10^{16}$	
Cryoplast SP15-1	$2,4.10^{19}$	$3,7.10^{16}$ ; $7,4.10^{15}$	
* $S_2$ - concentration of SC in the region g - 2			

High values of spin density can determine the plasticizing properties of the additives under study.

## 4. CONCLUSIONS

- Electron paramagnetic resonance (EPR) spectroscopy proved to be an effective method for characterizing paramagnetic centers in cement and cement-based systems without artificial induction of paramagnetism.
- An increase in the specific surface area of Portland cement particles led to a higher concentration of spin centers, which influenced hydration processes and strength development.
- The addition of activated Portland cement in the range of 5–15 wt.% resulted in an improvement in compressive strength, while higher contents caused a reduction in strength due to decreased density and less efficient particle packing.
- High-strength and rapid-hardening cements exhibited higher concentrations of spin centers and superior mechanical performance.
- A correlation between spin characteristics and the mechanical properties of cement-based materials indicates the possible involvement of radical and defect-related processes during hydration and hardening.

The individuality of EPR spectra allows this method to be considered as an express tool for binder identification and assessment of cement quality.

## FUNDING

None

## ACKNOWLEDGEMENT

The authors would like to thank the anonymous reviewers for their efforts.

## CONFLICTS OF INTEREST

The authors declare no conflict of interest

## REFERENCES

- [1] E. I. Shmitko, A. V. Krylova, and V. V. Shatalova, *Chemistry of Cement and Binders*. St. Petersburg, Russia: Prospekt Nauki, 2006, p. 206.
- [2] A. A. Pashchenko, *The Theory of Cement*. Kiev, Ukraine: Budivel'nik, 1991, p. 168.
- [3] V. B. Zakharov, S. G. Mamontov, and V. I. Sivoglazov, *Biology: General Patterns*. Moscow, Russia: School-Press, 1996, p. 614.
- [4] V. I. Vereshchagin and Yu. S. Sarkisov, "Using the patterns of geochemical processes in technologies of artificial materials," *Bulletin of the Tomsk Polytechnic University*, vol. 315, no. 3, pp. 12–15, 2009.
- [5] Yu. S. Sarkisov and T. V. Kuznetsova, "Synergetics and principles of non-equilibrium building materials science," *Tekhnika i Tekhnologiya Silikatov*, no. 4, pp. 2–6, 2009.
- [6] Yu. M. Bazhenov, V. S. Demyanova, and V. I. Kalashnikov, *Modified High-Quality Concrete*. Moscow, Russia: ASV Publishing House, 2006, p. 368.
- [7] B. Prokopets, "Influence of mechanoactivation effect on the activity of binders," *Building Materials*, no. 9, pp. 28–29, 2003.
- [8] V. Yu. Nesterov, Yu. V. Gavrilova, V. L. Khvastunov, Yu. S. Kuznetsov, and A. A. Krasnoshchekov, "Mechanochemical activation of silicite geosynthetic compositions," in *Proc. Int. Scientific and Technical Conf. Composite Construction Materials: Theory and Practice*, Penza, Russia, 2006, pp. 172–175.
- [9] Yu. S. Sarkisov, "Management of processes of structure formation of dispersed systems," *Izvestiya Vuzov. Building*, no. 2, pp. 106–109, 1993.
- [10] N. P. Gorlenko and Yu. S. Sarkisov, *Low-Energy Activation of Dispersed Systems*. Tomsk, Russia: Publishing House of Volga State University of Architecture and Building, 2011, p. 264.
- [11] I. G. Richardson, "The nature of C–S–H in hardened cements," *Cement and Concrete Research*, vol. 29, pp. 1131–1147, 1999.
- [12] K. Johansson, C. Larsson, O. N. Antzutkina, W. Forsling, H. R. Kotab, and V. Ronin, "Kinetics of hydration reactions in cement paste with mechanochemically modified cement: A  $^{29}\text{Si}$  MAS NMR study," *Cement and Concrete Research*, vol. 29, pp. 1575–1581, 1999.
- [13] J. Skibsted and C. Hall, "Characterization of cement minerals, cements, and their reaction products at the atomic and nano scale," *Cement and Concrete Research*, vol. 38, pp. 205–225, 2008.
- [14] T. Zhang, Q. Yu, J. Wei, and P. Zhang, "A new gap-graded particle size distribution and its influence on the properties of blended cement," *Cement and Concrete Composites*, vol. 33, pp. 543–550, 2011.
- [15] Yu. M. Butt and V. V. Timashev, *Portland Cement*. Moscow, Russia: Stroyizdat, 1974, p. 328.

- [16] L. Lapcik and Z. Simek, "Electron paramagnetic resonance study of dry cements," *Cement and Concrete Research*, vol. 26, no. 2, pp. 237–242, 1996.
- [17] E. A. Lopanova, "Radiospectroscopic studies of the hydration process of silicates using spin labels," *Problems of Materials Science*, no. 3, pp. 34–41, 2004.
- [18] D. A. Afanasyev, L. V. Tsyro, A. F. Unger, L. N. Andreeva, S. Ya. Aleksandrova, and F. G. Unger, "Spin aspects in the nature of cement hardening processes," *Polzunovskii Vestnik*, no. 3, pp. 82–85, 2009.